Structural Optimization with Aeroelastic Constraints of Rotor Blades with Straight and Swept Tips

R. Celi*
University of Maryland, College Park, Maryland 20742
and
P. P. Friedmann†
University of California, Los Angeles, California 90024

This paper describes a study in which structural optimization techniques are used to minimize the n/rev vertical hub shears in forward flight, subject to aeroelastic stability constraints in hover and frequency placement constraints. A special technique is used to build a sequence of approximate inexpensive to solve optimization problems, the solutions of which converge to the solution of the exact expensive to solve optimization problem. Blade configurations with both straight and swept tips, and single- and double-cell cross sections are analyzed. The results show that the approach used in this study is very efficient and produces improved designs with a very small number of blade aeroelastic analyses.

Nomenclature

b = blade semichord
C_T = thrust coefficient
$\boldsymbol{D}$ = vector of design variables
$f(\boldsymbol{D})$ = objective function
$\nabla F(\boldsymbol{D})$ = gradient of objective function or behavior constraints
$\boldsymbol{g}(\boldsymbol{D})$ = vector of behavior constraints
h_s = height of the single cell cross section
$[H(\boldsymbol{D})]$ = Hessian of objective function or behavior constraints
I_b = mass moment of inertia of the blade in flapping
J = mass polar moment of inertia of the rotor
ℓ = length of the elastic portion of the blade
t_1 = thickness of the cross section
V_{zpk} = peak-to-peak value of the 4/rev vertical hub shears, nondimensionalized through division by $2\Omega^2 I_b/\ell$
x_A = offset between the elastic axis and the aerodynamic center, positive for aerodynamic center ahead of the elastic axis
x_I = offset between the elastic axis and the center of gravity, positive for center of gravity ahead of the elastic axis
x_1 = distance between leading edge and internal wall in double cell cross section
x_2 = chordwise length of the cross section
γ = blade Lock number
ζ_k = real part of hover stability eigenvalue for the kth mode
Λ = tip sweep angle, positive for backward sweep
μ = advance ratio
σ = rotor solidity
Ω = rotor angular velocity

Introduction

ONE of the most cost-effective solutions to the problem of vibration in rotorcraft is to design rotor blades with an inherently low vibration level. This can be accomplished by aeroelastic tailoring the blade, using structural optimization. This implies that the blade mass and stiffness distributions and its geometry are determined in such a manner that the vibration levels at the rotor hub are minimized. In this paper, the word "optimization" indicates an approach in which the design problem is cast in mathematical programming form, and does not include, for example, studies in which the best design is chosen as the result of parametric studies.

A thorough review of the literature concerning the use of optimum design techniques in dynamic problems, and particularly in helicopter rotor blade dynamic design, is presented in Ref. 1. A more recent survey has been presented by Friedmann.[2] These reviews reveal the existence of a very limited amount of work devoted to the structural optimization of rotor blades for vibration reduction.

In another recent survey, Miura[3] states that it is not unreasonable to pursue design optimization in areas, such as helicopter vibration reduction, in which reliable prediction capabilities do not exist yet. Better optimization technology can be developed and implemented in highly modular computer codes so that new improved analysis codes can be easily incorporated as they become available, and the optimization program can work with the best predictive capability available at any particular time.

When the mass and stiffness distributions of the blade are changed to reduce the vibration levels, it is very important to be sure that no degradation of the aeroelastic stability occurs. This is even more important when tip sweep is added as a design variable, because of its powerful influence on both blade response and stability.[4] Prudence mandates the introduction of aeroelastic stability constraints in the optimum design process. This complicates the design problem because a fully coupled aeroelastic stability and response analysis has to be combined with the structural optimization program. Only a few studies having this capability are available.[1,5,6] In Refs. 1,

Presented as Paper 88-2297 at the AIAA/ASCE/AHS 29th Structures, Structural Dynamics and Materials Conference, Williamsburg, VA, April 18-20, 1988; received Aug. 2, 1988; revision received May 15, 1989.

*Assistant Professor of Aerospace Engineering, Center for Rotorcraft Education and Research, Department of Aerospace Engineering. Member AIAA.

†Professor and Chairman, Mechanical, Aerospace, and Nuclear Engineering Department. Associate Fellow AIAA.

5, and 6, the objective was the minimization of the 4/rev oscillatory vertical hub shears at an advance ratio $\mu = 0.3$. The aeroelastic stability constraints required that the hover stability not be degraded by more than a specified amount in the course of the optimization process. Additional constraints required that the fundamental frequencies in flap, lag, and torsion fell between the preassigned upper and lower bounds.

In a study by Peters et al.,[7] two different objective functions were used, to minimize blade weights in one case and the discrepancy between desired and actual natural frequencies of the blade. A simplified forced response analysis leads the authors to conclude that the objective functions used in the study are "adequate" for vibration reduction purposes, but no comprehensive aeroelastic analysis is performed and no stability constraints are imposed on the design.

Davis and Weller[8] used structural optimization technique to solve four different dynamic problems, namely: 1) maximization of the in-plane structural damping of a bearingless rotor with elastomeric dampers; 2) placement of blade natural frequencies; 3) minimization of the vibratory hub shears using a simplified rotor aerodynamic model; and 4) minimization of certain rotor vibration indices. The rotor analysis codes were directly coupled to the optimization codes. No aeroelastic stability constraints were considered.

A serious problem encountered in the direct coupling of a comprehensive aeroelastic stability and response analysis code with an optimization, or nonlinear mathematical programming code is the very large computational effort required for the solution. This problem can be alleviated by constructing an *approximate*, computationally easier to solve, optimization problem.[9] The approximate problem is updated frequently, so that the sequence of solutions of the approximate problems converges to the solution of the original exact optimization problem.

One typical method of constructing the approximate problem is to expand the objective function and the behavior constraints in first- or second-order Taylor series in terms of the design variables, and in the neighborhood of the current design.[9] This method originated in the field of static structural analysis, in which the gradient information required to construct the Taylor series expansions can be obtained at a fraction of the cost of one analysis, through implicit differentiation.[10] This is difficult to achieve in helicopter aeroelastic optimizations, and the gradient information has to be constructed using expensively computed finite difference approximations. References 1, 5, and 6 utilized an expensive approach based on finite differences for generating approximations to the objective function and aeroelastic constraints. The generation of the approximations problem was cumbersome and had to be carried out in an interactive manner during the optimization process. It is also possible to construct approximate problems using derivatives, or the sensitivity of the objective function. A sensitivity study that is potentially useful in this context has been carried out by Lim and Chopra.[11]

This paper has two main objectives:

1) To present a new formulation of the structural optimization problem for a helicopter rotor blade in forward flight. The objective is the minimization of the n/rev vertical hub shears. The behavior constraints express mathematically the requirements that the blade be aeroelastically stable, that its natural frequencies fall between preassigned upper and lower bounds, and that the autorotation performance not be degraded during the aeroelastic tailoring process. A new formulation of the approximate problem allows increase in efficiency, in the complete solution of the optimum design problem, of at least one order of magnitude, compared with existing procedures.

2) To present results obtained by letting the *tip sweep angle* be one of the design variables in the optimization procedure. Tip sweep has a powerful influence on the dynamic behavior of the blade, and when included in the aeroelastic tailoring process can lead to further reductions in blade vibration levels.

Aeroelastic Stability and Response Analysis

This section describes briefly the aeroelastic stability and response analysis and the procedure to calculate the vertical hub shears, that is, the analysis portion of the optimum design process. The equations of motion of the straight blade are similar to those derived in Ref. 12. The modeling of the swept tip is described in Ref. 4. The equations describe the coupled flap-lag-torsional motion of a flexible homogeneous isotropic blade, modeled as a Bernoulli-Euler beam undergoing small strains and moderate deflections. Geometrically nonlinear terms are present in the structural, inertia, and aerodynamic operators, due to nonlinear beam kinematics. The inertia loads are obtained using D'Alembert's principle. Quasisteady strip theory, with uniform inflow, is used to derive the aerodynamic loads. Stall and compressibility effects are not included. In the modeling of the swept tip, the independence principle is assumed to apply, that is, the aerodynamic loads depend only on the component of the flow contained in the plane of the cross section, and radial flow effects are neglected.[4]

The spatial dependence of the partial differential equations of motion of the blade is eliminated by using a Galerkin method of weighted residuals.[12] This results in a finite element discretization. Cubic interpolation polynomials are used for the modeling of flap and lag bending, quadratic interpolation polynomials for the modeling of torsion. The resulting finite elements have a total of 11 degrees of freedom: displacement and slope at each end of the element for flap and lag bending, rotation at each end of the element and at a midelement node for torsion. The axial degree of freedom is eliminated by making the assumption that the blade is inextensional. The partial differential equations of motion of the blade are, thus, transformed into a set of nonlinear coupled ordinary differential equations with periodic coefficients. A modal coordinate transformation is performed to reduce the number of degrees of freedom. Six rotating coupled blade normal modes are used to perform the modal coordinate transformation. The coupled modes are calculated for a root pitch angle equal to the collective pitch.

In forward flight, the equilibrium position of the blade is time dependent and is obtained by solving a sequence of linear periodic response problems using quasilinearization. The stability of the system is determined using the Floquet theory. A special implicit formulation of quasilinearization[13] that reduces considerably the implementation effort is used. The algebraic expressions that define the aerodynamic loads are not expanded explicitly. They are coded separately in the computer program and combined numerically during the solution procedure. Quasilinearization is a Newton-Raphson type procedure, and the derivative matrices that are required by the algorithm are computed using finite-difference approximations.

The overall helicopter trim procedure used in this study is a propulsive trim procedure identical to that used in Ref. 14.

The calculation of the hub loads—forces and moments— is performed using the direct force integration method. The response of the blade is provided by the aeroelastic response calculation code in the form of azimuthwise Fourier series expansions of the generalized coordinates. The calculation of the hub loads then proceeds as follows:

1) Aerodynamic and inertia loads are calculated at a certain number of azimuth angles and spanwise stations of a reference blade.

2) Aerodynamic and inertia root loads for the reference blade are computed in the rotating coordinate system, using a numerical spanwise integration of the local loads. The root loads are functions of azimuth only and are expanded in Fourier series.

3) Fourier expansions of the total hub loads in the nonrotating coordinate system are obtained by summing the inertia and aerodynamic contributions from all the blades. The assumption is made that all the blades are identical and perform

identical motions. Thus, the loads on all the blades are known once the loads on the reference blade are known.

The details of the numerical integration procedures and of the Fourier series expansions, as well as of the various coordinate transformations required for the calculation of the hub loads, are omitted in this paper for brevity; they can be found in Ref. 15.

Formulation of the Optimum Design Problem

The optimization problem is cast in nonlinear mathematical programming form. Thus, the objective is to minimize a function $f(\boldsymbol{D})$ of a vector $\boldsymbol{D}$ of design variables, subject to a certain number of constraints $g(\boldsymbol{D}) \leq 0$

$$\text{minimize } f(\boldsymbol{D}) \tag{1}$$

subject to

$$g(\boldsymbol{D}) \leq 0 \tag{2}$$

To reduce the computational requirements, the computer program performing the aeroelastic analysis is not connected directly to the optimization program. Instead, the optimization is conducted on an *approximate problem*, which reproduces the characteristics of the actual problem in a neighborhood of the current design, and which is continuously updated as the optimization progresses.

An effective method of building an approximate problem is to expand the objective function and the behavior constraints in Taylor series in terms of the design variables[9]

$$F(\boldsymbol{D}) \approx F(\boldsymbol{D}_0) + \nabla F(\boldsymbol{D}_0)^T \delta \boldsymbol{D} + \frac{1}{2} \delta \boldsymbol{D}^T [H(\boldsymbol{D}_0)] \delta \boldsymbol{D} \tag{3}$$

where $F(\boldsymbol{D})$ is taken to be any objective or constraint function, $\boldsymbol{D}_0$ is the current design, and $\nabla F(\boldsymbol{D}_0)$ and $[H(\boldsymbol{D}_0)]$ are, respectively, the gradient and Hessian matrix at the current design. The Hessian matrix is the matrix of the second partial derivatives of the objective function, with respect to the design variables. The perturbation vector $\delta \boldsymbol{D}$ is defined as

$$\delta \boldsymbol{D} = \boldsymbol{D} - \boldsymbol{D}_0 \tag{4}$$

The most expensive function to evaluate is the objective function. The cost of one evaluation of the objective function is two orders of magnitude higher than the total cost of evaluating the behavior constraints. No analytic expressions for the gradients are available for the objective function, and finite difference approximations are required for the construction of the derivative information in Eq. (3). Therefore, if n design variables are used in the optimization, n additional aeroelastic analyses are required to compute the gradient, and an additional $n(n+1)/2$ for the calculation of the Hessian, making the cost of building the Taylor series approximation to the objective function extremely high. For this reason an alternative approximation technique, introduced by Vanderplaats,[16,17] was used in this study.

This alternative technique is based on the idea of approximating the gradient and the Hessian in Eq. (3), not by using small finite difference steps, but by using whatever design information is available at the time. Eq. (3) can be rewritten, in expanded form, as [16,17]

$$\begin{aligned}\Delta F = {} & \nabla F_1 \delta D_1 + \nabla F_2 \delta D_2 + \ldots + \nabla F_n \delta D_n \\ & + \frac{1}{2}(H_{11}\delta D_1^2 + H_{22}\delta D_2^2 + \ldots + H_{nn}\delta D_n^2) \\ & + H_{12}\delta D_1 \delta D_2 + H_{13}\delta D_1 \delta D_3 + \ldots + H_{1n}\delta D_1 \delta D_n \\ & + H_{23}\delta D_2 \delta D_3 + \ldots + H_{n-1,n}\delta D_{n-1}\delta D_n\end{aligned} \tag{5}$$

in which

$$\Delta F = F(\boldsymbol{D}) - F(\boldsymbol{D}_0) = F - F_0 \tag{6}$$

and

$$\nabla F_i = \nabla F_i(\boldsymbol{D}_0) \qquad H_{ij} = H_{ij}(\boldsymbol{D}_0) \tag{7}$$

Assume that a baseline design $\boldsymbol{D}_0$ has been analyzed to give F_0 and that other designs $\boldsymbol{D}_1$, $\boldsymbol{D}_2$,.., $\boldsymbol{D}_k$ have been previously analyzed to provide F_1, F_2,..., F_k. Let

$$\delta \boldsymbol{D}_i = \boldsymbol{D}_i - \boldsymbol{D}_0 \qquad i = 1,2,\ldots, k \tag{8}$$

and

$$\Delta F_i = F_i - F_0 \qquad i = 1,2,\ldots, k \tag{9}$$

If k designs are available, Eqs. (5) can be written k times. The unknowns of the resulting linear system are ∇F_1, $\nabla F_2,\ldots,\nabla F_k$, and H_{11}, $H_{12},\ldots,H_{nn}$. If exactly $l = 1 + n + n(n+1)/2$ designs are available, and if all the designs are linearly independent, the system of l [Eqs. (5)] will provide all the coefficients required for the quadratic polynomial approximation Eq. (3). If all the designs are very closely spaced, the solution of the system of Eqs. (5) will provide the finite-difference approximations to gradient and Hessian matrix at $\boldsymbol{D}_0$. Equation (3) will then represent a truncated Taylor series expansion of F, valid in a neighborhood of $\boldsymbol{D}_0$. If the designs are dispersed in the design space, Eq. (3) will simply be a quadratic polynomial approximation, defined over a wider region of the design space.

An important characteristic of this technique is that the system of Eqs. (5) can be written with less than l equations. If at least $n + 1$ designs are available, the solution of the system will provide the linear portion of the approximation, Eq. (3). An approximate optimization can be conducted, based on this linear approximation. The resulting optimum is then analyzed precisely and provides an additional design: a system of $n + 2$ [Eqs. (5)] can then be written. Its solution will provide a new approximation, Eq. (5), with all the linear terms plus one pair of quadratic terms of the symmetric Hessian matrix. The process can then be repeated, with each new approximate optimum providing an additional design point to increase the number of terms in the quadratic approximation to objective function and behavior constraints.

One iteration of the optimum design process, thus, consists of the following six steps:

1) calculation of the blade properties, including natural frequencies and mode shapes;

2) aeroelastic analysis in hover;

3) aeroelastic analysis in forward flight, including calculation of hub loads;

4) calculation of objective function and behavior constraints;

5) calculation of a new approximation (linear or incomplete quadratic) to objective function and behavior constraints; and

6) solution of the approximate constrained optimization problem, using the feasible direction code CONMIN,[19] to obtain a new, improved blade design.

The process is terminated when a feasible optimum design has been reached, or, arbitrarily, when the improvement in the design is considered "adequate."

The first $n + 1$ iterations of the procedure are not true optimization iterations, because steps 5 and 6 above are not performed. In fact, these initial iterations are used to generate a sufficient number of designs to build at least an initial linear approximation to objective function and behavior constraints.

Side constraints are placed on the design variables to prevent them from reaching impractical values that violate practical physical constraints. Thus, all the thicknesses and distances are assumed to be non-negative numbers. No side

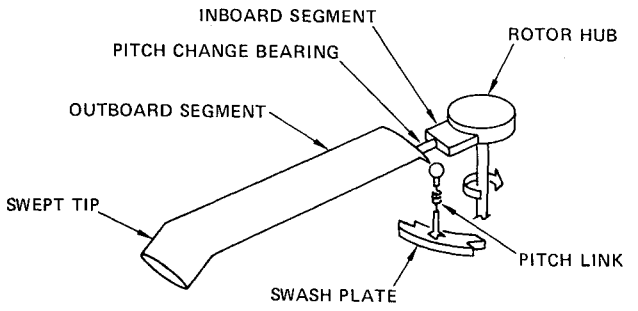

Fig. 1 Swept tip hingeless rotor blade model.

constraints were placed on the tip sweep angle Λ, which could assume positive (swept back tip) or negative angles, as determined by the optimizer.

Three different types of *behavior constraints* are placed on the design:

1) *Frequency placement constraints*. The fundamental frequencies in flap, lag, and torsion are required to fall between preassigned upper and lower bounds. If ω is one of the three frequencies, and ω_L and ω_U are the preassigned lower and upper bound, respectively, the frequency placement constraint is expressed mathematically in the form:

$$g(\boldsymbol{D}) = \frac{\omega^2}{\omega_U^2} - 1 \leq 0 \tag{10}$$

$$g(\boldsymbol{D}) = 1 - \frac{\omega^2}{\omega_L^2} \leq 0 \tag{11}$$

Eqs. (10) and (11), written for each of the three fundamental frequencies of the blade in flap, lag, and torsion, provide a total of six behavior constraints.

2) *Aeroelastic stability constraints*. The blade is required to be aeroelastically stable in hover. No constraints are placed on the stability in forward flight, because all the blade configurations considered in this optimization study are soft-in-plane blade configurations, and the effect of forward flight is usually stabilizing for this type of blade.[14] The aeroelastic stability constraints are expressed mathematically in the form

$$g(\boldsymbol{D}) = \zeta_k \leq 0 \qquad k = 1, 2, \ldots, m \tag{12}$$

If m modes are used to perform the modal coordinate transformation in the solution of the equations of motion, there are m constraint equations, like Eq. (12), where the quantity ζ_k is the real part of the hover stability eigenvalue for the kth mode.

3) *Autorotation constraint*. The autorotation constraint expresses the requirement that possible mass redistributions produced in the optimization process do not degrade the autorotation properties of the rotor. Several indices have been formulated to provide a measure of the autorotation qualities of a helicopter (Ref. 20, pp. 346-364). Of all the parameters that may affect such qualities, the only one that could be changed during the optimization process considered in this study is the mass polar moment of inertia of the rotor. Therefore, the autorotation constraint is expressed mathematically in the form

$$g(\boldsymbol{D}) = 1 - \frac{J}{0.9J_0} \leq 0 \tag{13}$$

The constraint Eq. (13) requires that the mass polar moment of inertia J of the rotor maintain, during the optimization, at least 90% of its initial value J_0.

Therefore, *a total of 13 behavior constraint equations* are placed on the design variables.

Results

The basic blade configuration considered in this study is a soft-in-plane hingeless blade configuration, sketched in Fig. 1, with uncoupled fundamental lag, flap, and torsion frequencies for zero tip sweep of 0.732/rev, 1.125/rev, and 3.17/rev, respectively. The Lock number is $\gamma = 5.5$, the thrust coefficient $C_T = 0.005$, and the rotor solidity $\sigma = 0.07$. For the swept tip configurations, the outermost 10% of the blade is swept. The blade precone angle β_p, the root offset e_1, the offset x_A between the elastic axis and the aerodynamic center, and the offset x_I between the elastic axis and the cross-sectional center of gravity are all set to zero, unless specified otherwise. The modal coordinate transformation is based on the six lowest frequency rotating coupled modes of the blade. In all cases, the six modes were one torsion, two lag, and three flap modes. The blades were modeled using five finite elements, with nodes at 0%, 22.5%, 45%, 67.5%, 90%, and 100% of the span. Selected results are presented here. Numerous additional results can be found in Ref. 15.

Two types of cross sections are considered in this study, namely a single cell rectangular cross section and a double cell cross section are composed. Both cross sections are shown in Fig. 2. Up to five and up to nine independent design parameters can be specified for the single cell and the double cell cross section, respectively.[15] In this study, the cross-sectional design parameters are linked in such a way as to reduce the number of independent design parameters to two, for both the single and the double cell cross sections. The first independent design variable is the thickness t_1 of all the elements of which both cross sections are composed. In the single cell cross section, the ratio between the width x_2 and the height h_s is kept constant, with $x_2/h_s = 4.5$. In the double cell cross section, the internal wall is placed halfway between the leading edge and the rear wall, so that $x_1 = x_2/2$. The outside the wall of the double cell cross section has the shape of a NACA 0012 airfoil. The properties of both cross sections are presented in Ref. 15.

As a preliminary to the optimization studies, the effect of tip sweep on the peak-to-peak values of the 4/rev vertical hub shears was investigated. Figure 3 shows the peak-to-peak value V_{zpk} of the vertical hub shears as a function of the tip sweep angle Λ, for four different values of the advance ratio μ. Figure 3 shows that tip sweep may or may not be beneficial for the soft-in-plane configuration, depending on the advance ratio and the tip sweep angle. At an advance ratio $\mu = 0.3$, the oscillatory loads rapidly increase with tip sweep. At $\mu = 0.4$, instead, tip sweep has a beneficial effect. Based on the results of this preliminary investigation, the advance ratio at which the 4/rev vertical hub shears were to be minimized was set at $\mu = 0.4$.

Three optimization studies were conducted using the general procedure outlined in the previous section, namely:

1) Case 1: Optimization of a completely straight blade, having a two-cell cross section. The objective function is the peak-to-peak value of the 4/rev vertical hub shears at an

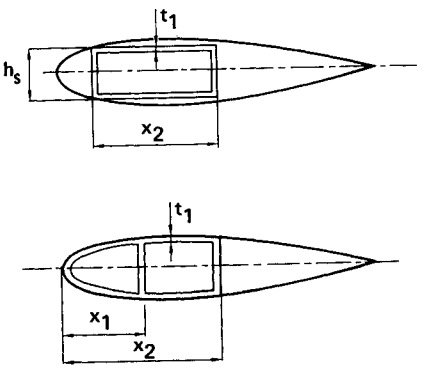

Fig. 2 Single- and double-cell cross sections.

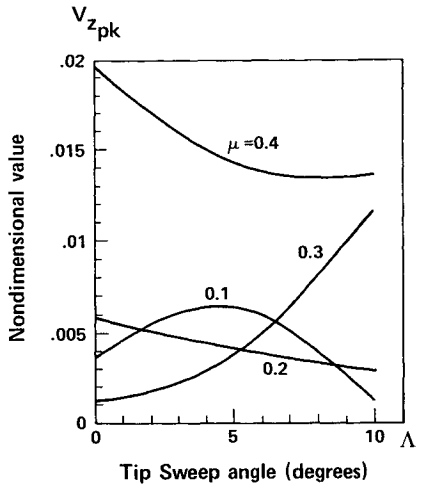

Fig. 3 Effect of tip sweep on the peak-to-peak value of the vertical hub shears, soft-in-plane blade configuration.

advance ratio $\mu = 0.4$. Because the cross section is not doubly symmetric, the blade generally has nonzero values of the aerodynamic center-elastic axis offset x_A and of the center of gravity-elastic axis offset x_I.

The design variables are defined at three distinct cross sections of the blade: the root section, the tip section, and the cross section at the 67% span, *for a total of six individual design variables*. The 67.5% station, at which two design variables are defined, is the junction section between the third and the fourth finite element. The blade properties are assumed to vary linearly between two consecutive stations at which the design variables are specified.

2) Case 2: Optimization of the completely straight blade, having a single cell cross section. As in the previous case, the objective function is the peak-to-peak value of the 4/rev vertical hub shears at an advance ratio $\mu = 0.4$.

As in case 1, the design variables are defined at three distinct cross sections of the blade: the root section, the tip section, and the cross section at the 67.5% span, *for a total of six independent design variables.*

The cross section is rectangular, therefore, doubly symmetric. Because leading edge masses have not been used in this particular example, the center of gravity and the aerodynamic center are located on the elastic axis of the blade—which is taken to be coincident with the pitch axis. Therefore, the associated offsets are equal to zero.

3) Case 3: Optimization of a straight blade with a swept tip. The objective function is the peak-to-peak value of the 4/rev vertical hub shears divided by the thrust coefficient C_T, at an advance ratio $\mu = 0.4$. This particular choice of objective function is an attempt to compensate for the inaccuracy of the trim program, which neglects the torsional deformation of the blade, and, thus, overestimates the thrust that the rotor is actually capable of developing.

The outermost 10% of the blade is swept, with the sweep angle being a design variable of the optimization procedure. The cross section is rectangular, and, therefore, the offsets x_I and x_A are equal to zero. The cross-sectional design variables are defined, as in case 2. Therefore, a *total of seven design variables* is used in this case.

The initial blade configuration, for all three cases, is the baseline soft-in-plane configuration.

Optimization Case 1

The iteration history of the objective function for case 1 is shown in Fig. 4. It should be noted that for all three optimization cases, design n is defined as the design produced at the end of the optimization step n. Furthermore, in all the results of this study, the values of the flapping inertia I_b used to nondimensionalize the vertical hub shears are those corresponding to the respective *baseline* blade configurations. Step 0 and the first six steps are not true optimization steps; they are required to obtain enough information to build linear approximations to the objective function and behavior constraints. Step 0 is the analysis of the baseline design. In steps 1 through 6, each of the six design variables is perturbed, one at a time. Because the perturbations were relatively small—1% of the baseline value—the linear approximations obtained at the end of step 6 can be considered as gradients, calculated using forward finite-difference approximations.

Step 7 is the first true optimization step and consists of the solution of a linear optimization problem. Move limits were placed on the design variables, which would not change by more than 25% of the baseline value. The optimization continues for three additional steps (8-10). Each new proposed design is analyzed precisely and used to improve the polynomial approximations to objective function and behavior constraints. The diagonal of the Hessian matrix is built first, as more function evaluations become available. (The term "Hessian" is used in this section with the general meaning of "matrix of coefficients of the quadratic terms of the approximation.") Figure 4 shows that, after reaching a minimum at step 8, the objective function slightly oscillates.

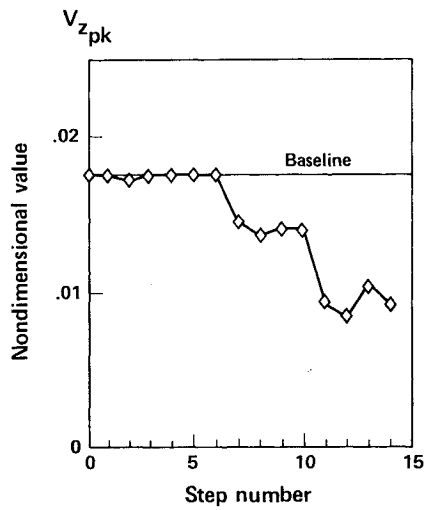

Fig. 4 Case 1—iteration history of the objective function: $C_T/\sigma = 0.07$, $\mu = 0.4$.

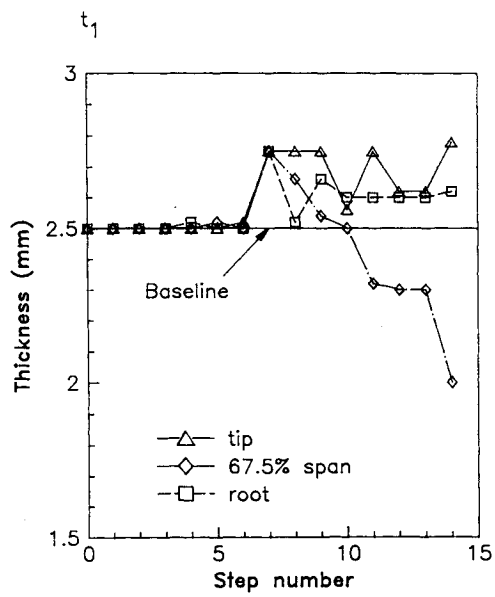

Fig. 5 Case 1—iteration history of thickness t_1.

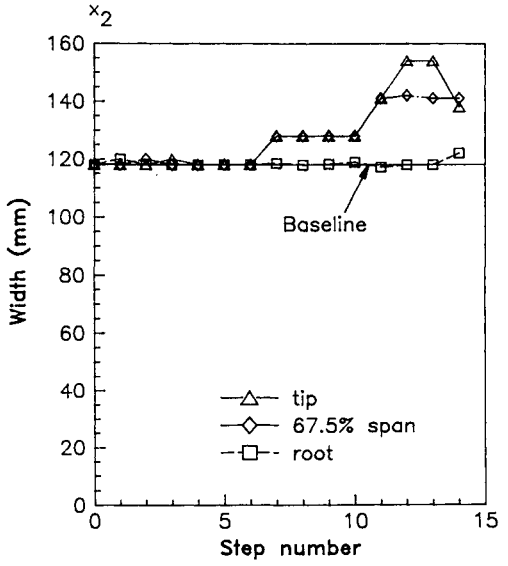

Fig. 6 Case 1—iteration history of chordwise width x_2.

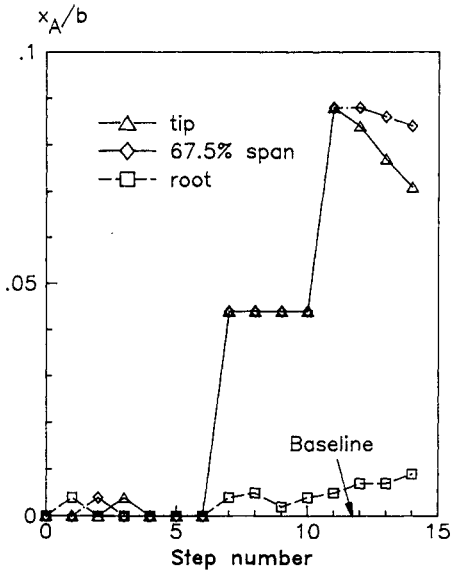

Fig. 7 Case 1—iteration history of aerodynamic center-elastic axis offset x_A.

At the constrained optimum of the approximate problem, the approximate flap damping constraint for the first flap mode was active. In most helicopter blades, the first flap mode tends to be highly damped, and a precise analysis of the proposed design showed that this indeed was the case, and that the precise first flap stability constraint was satisfied. The constraint was, therefore, reformulated as

$$\zeta_{F1} - 0.3 < 0 \tag{14}$$

The subsequent optimization steps were performed with this new form of the constraint, which prevents the *approximate* constraint from becoming critical. Two more steps (11 and 12) are performed with the relaxed flap constraint. The design of step 12 is a local unconstrained minimum of the approximate problem. The corresponding blade is such that a reduction of 54.3% is achieved in the objective function, compared with the baseline configuration. The design suggested by the optimizer for step 13 is practically the same as that for step 12. A different design was, instead, arbitrarily selected for step 13. This design was "close" to that of step 12 and was selected solely for the purpose of adding one design to the design data base and trying to improve the accuracy of the approximations in the neighborhood of design 12—with the design of step 13 the full diagonal of the Hessian can be built. Step 14 is the last optimization step, and it produces a value of the objective function that is slightly higher than the minimum of step 12. The optimization was arbitrarily stopped at this point. All the designs generated during the optimization were feasible. With the only exception the damping constraint on the first flap mode at step 10, no behavior constraints were active.

The iteration history of the *design variables* is presented in Figs. 5 and 6. Figure 5 contains three plots, one for the value of the thickness t_1 at each of the three preassigned spanwise stations and shows that the optimizer designs a blade that is thicker than the baseline at the root and the tip and thinner at the 67.5% station. Figure 6 shows, for each of the three blade stations, the chordwise extension of the two-cell spar. (Recall that the front internal wall is located halfway between the leading edge and the rear internal wall.) Figure 6 shows that the optimizer makes the structural cross section wider and, therefore, stiffer, going from the blade root toward the tip.

Figure 7 shows the iteration history of the *cross-sectional offset* between the elastic axis and the aerodynamic center. The relative placement of these points is not a design variable, but is affected by the values of the design variables because the cross section is not doubly symmetric. Figure 7 shows that, as the optimization progresses, a relatively large forward shift of the aerodynamic center is introduced in the outboard portion of the blade. The offset is about 4% of the blade chord at the optimum for the tip section. The baseline design has a slightly forward placed center of gravity ($x_I = 0.0014\ell$), and the optimizer moves it further forward by small amounts. The iteration history of x_I is not presented here for the sake of brevity and can be found in Ref. 15.

Optimization Case 2

The iteration history of the *objective function* for case 2 is shown in Fig. 8. Steps 0 through 6 are not true optimization steps. These steps are required to generate enough designs to construct at least linear approximations to objective function and behavior constraints. The design at step 0 is the baseline blade design. The designs analyzed in steps 1 through 6 are obtained by changing one design variable at the time. Since the change in each variable was equal to 10% of its baseline value, the resulting linear approximations to objective functions and behavior constraints cannot be strictly considered as gradients.

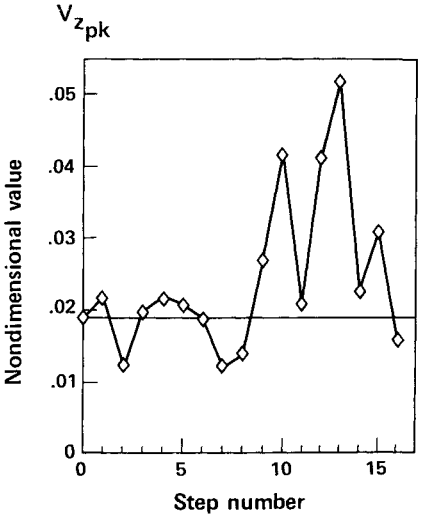

Fig. 8 Case 2—iteration history of the objective function: $C_T/\sigma = 0.07$, $\mu = 0.4$.

The first true optimization step is step 7, which consists of a linear constrained optimization problem. A reduction of 37.6% is achieved, compared with the baseline design. In the next step, the objective function increases slightly. Because this behavior is somewhat similar to the one observed in case 1, the optimization was arbitrarily concluded at this point and restarted *with a new set of behavior constraints*.

The aeroelastic stability constraints used in case 1, and up to this point in case 2, consist of requiring that the blade be aeroelastically stable in hover. It is prudent to require that the optimization process should not degrade too much the stability of the baseline design. The optimization was, thus, restarted from step 9 with these more stringent behavior constraints. The aeroelastic constraints of Eq. (12) are reformulated as

$$g(\boldsymbol{D}) = 1 - \frac{\zeta_k}{0.95\zeta_{kB}} \leq 0 \qquad k = 1, 2, \ldots, m \qquad (15)$$

Eq. (15) expresses the requirement that the loss of stability of a given mode should not exceed 5% of the baseline value ζ_{kB}.

The optimization is not restarted with a new calculation of an initial linear approximation. Rather, the previous designs are reused to provide the initial approximation for the new case. Although designs 0 through 8 were all feasible with respect to the old set of behavior constraints, some of these designs are now infeasible with respect to the tightened aeroelastic stability constraints. In particular, design 8, which becomes the initial design for the second phase of this optimization, is infeasible.

The first design produced by the optimizer with the new set of constraints is feasible with respect to the *approximate* behavior constraints. When this design is analyzed precisely, it proves to be infeasible with respect to the *exact* behavior constraints. The successive design (step 10) is feasible with respect to both the approximate and the exact behavior constraints. The next design (step 11) is again feasible with respect to the approximate, but not the exact, behavior constraints. In steps 9 through 11, the objective function is constantly at a value higher than the baseline value, and does not show any signs of convergence to the optimum. In other words, the optimizer does not seem to be able to produce a feasible design that improves on the baseline design—which obviously satisfies the new constraint equations, Eq. (15).

The apparently erratic behavior of the objective function required a reconsideration of the optimization strategy that, starting from step 14, was modified as follows:

1) At each optimization step, take as the baseline design $\boldsymbol{D}_0$ the design with the lowest value of the objective function, whether or not that design is the latest analyzed, and whether or not that design is feasible. Impose relatively tight move limits on the design variables, for example, allowing a maximum change of 10% of the baseline value.

2) If the new design generated by the optimizer has a lower value of the objective function, use it as the starting point for the next optimization step. Otherwise, retain the new design, but again start the next optimization step with the design with the lowest value of the objective function. Tighten the move limits further.

3) When a good design is obtained, use it as the starting point for the next optimization step, and progressively widen the move limits.

4) If the design with the lowest value of the objective function is infeasible, and the optimizer consistently fails to produce a design that is both feasible and with a value of the objective function lower than that of the initial design, restart the optimization from the initial design. Do not discard any of the previous designs, unless enough function evaluations have already been performed to construct a complete quadratic approximation.

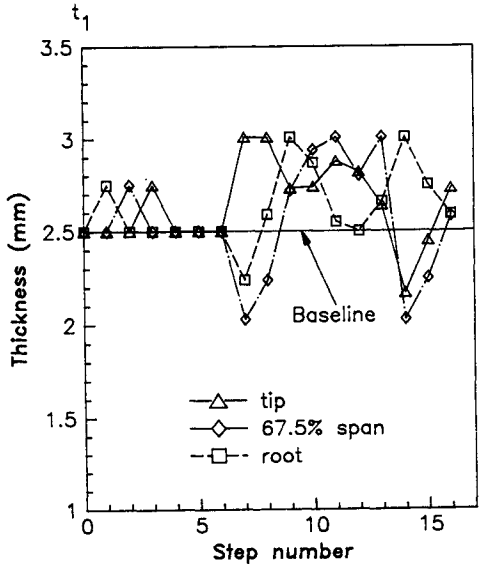

Fig. 9 Case 2—iteration history of thickness t_1; phase 2 (modified aeroelastic stability constraints) begins with step 9.

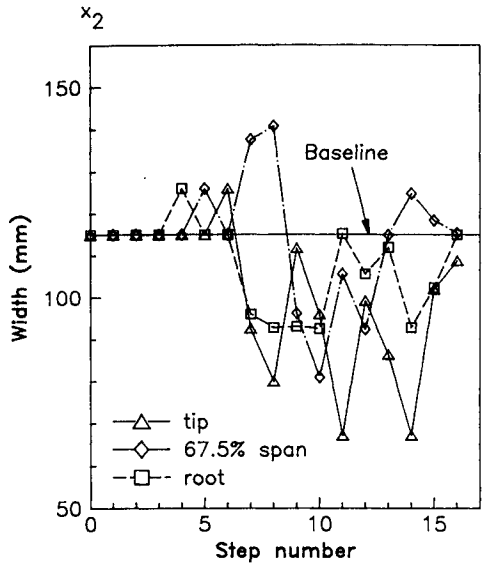

Fig. 10 Case 2—iteration history of chordwise width x_2.

The new strategy is applied starting with step 14, shown in Fig. 8. The starting design is design 2, which is infeasible and has the lowest value of the objective function. Move limits are placed on the design variables. The maximum allowable change is 10% of the values of design 2. The design produced by CONMIN is still infeasible, but already shows a large decrease in the objective function. The next step (step 15) again uses design 2 as the starting design. The same move limits as in the previous step are imposed. Design 15 is now feasible, although the objective function has increased. Step 16 again starts from design 2, but the move limits are tightened. A maximum change of only 5% in the value of the design variables is now allowed, with respect to design 2. The design produced by the optimizer has a value of the objective function that is still higher than that of design 2, but lower than the baseline value of design 0. Furthermore, design 16 is feasible, whereas design 2 was not. Design 16 is constrained by the move limits. The reduction in the peak-to-peak value of the 4/rev vertical hub shears is of 16.6%, compared with the baseline value. Thus, the imposition of the tightened aeroelastic constraints reduces the gains in the objective function by more than 50%.

This design is used as the starting design for step 17. The move limits are widened from 5% to 10%. The design produced by CONMIN is so close to that of step 16 that a new

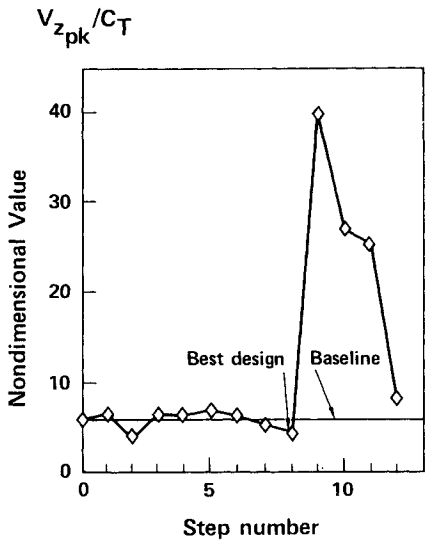

Fig. 11 Case 3—iteration history of the objective function: $C_T/\sigma = 0.07$, $\mu = 0.4$.

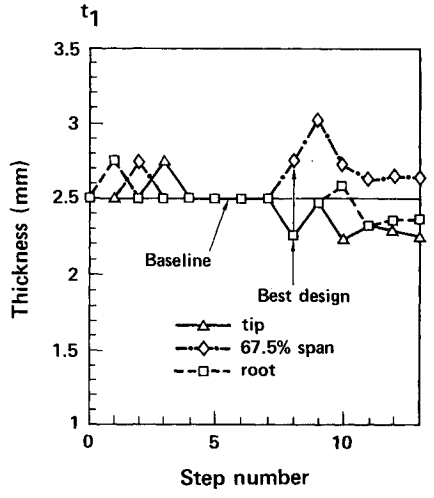

Fig. 12 Case 3—iteration history of thickness t_1.

precise analysis is not performed—for this reason step 17 is not included in Figs. 8–10. The design is now constrained by the *approximate* aeroelastic constraints. The first lag, second flap, and second flap constraints are active. The second lag constraint is slightly violated, but it remains within the narrow numerical band that straddles the exact value of the constraint. (Constraints are usually defined in CONMIN as narrow strips instead of strictly as lines.[18,19]) The side constraints are no longer active.

Design 17 is at least a local minimum for the approximate problem. It is not necessarily a local minimum for the exact problem. Whether or not this is the case depends on the quality of the approximations to objective function and behavior constraints. If it is important to get as close as possible to the local minimum of the exact problem, a certain number of designs should be analyzed in the neighborhood of the approximate minimum to improve the quality of the approximations, and the optimization should be continued with the improved approximations. Because some of the assumptions made in the derivation of the blade stability and response analysis are relatively crude, such refinements are not warranted, and the optimization is stopped at design 17.

Optimization Case 3

Figure 11 shows the iteration history of the objective function for case 3, which is the peak-to-peak value of the 4/rev vertical hub shears *divided by the thrust coefficient* C_T. The tightened aeroelastic constraints of Eq. (15) are enforced.

Design 0 is the baseline soft-in-plane straight blade configuration. The first seven steps are not true optimization steps. As in cases 1 and 2, they provide enough precise values of the objective function and behavior constraints to build at least a linear approximation of objective and constraints. In the designs 1–7, each of the seven design variables is perturbed, one at the time. Design 7 is the only swept blade design. Designs 0–6 are straight blade designs and are identical to the corresponding designs of case 2. Thus, these designs are not reanalyzed, and the values obtained in case 2 are reutilized. The swept tip blade of design 7 is one of the blade configurations analyzed to derive the results of Fig. 3 and need not be recalculated.

Thus, the optimization of case 3 begins without the need for any precise analyses, in the sense that the eight precise analyses required to start the procedure were already available from previous parts of this study and could be directly reutilized. The ability to make use of previously analyzed designs, even if not very close to the expected optimum in the design space of the current problem, is one of the most important features of the optimization algorithm used in this study.

The first true optimization step—step 8—produces a design with a reduction of 27.2% of the objective function, with respect to the baseline straight blade. This also corresponds to a reduction of 14.5% with respect to the best swept tip design obtained without applying formal optimization techniques, that is, design 7. When analyzed precisely, the design proves

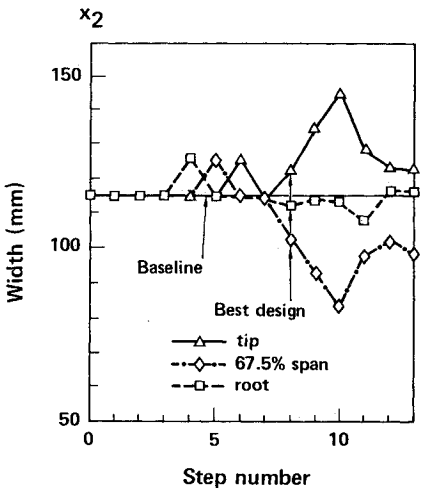

Fig. 13 Case 3—iteration history of chordwise width x_2.

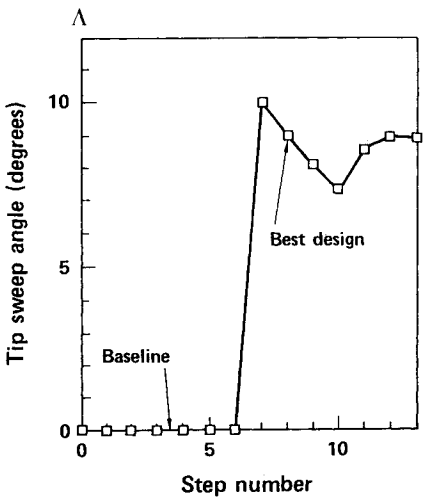

Fig. 14 Case 3—iteration history of tip sweep angle Λ.

feasible, with no constraints active. Compared with the final result of case 2, in which the blade is straight, the use of tip sweep as an additional design variable allows a further reduction of the objective function of almost 10%.

The next two steps (9 and 10) produce much higher values of the objective function. Starting with step 11, the "modified" strategy previously outlined is employed. The next two steps (11 and 12) provide considerable reductions of the objective function, but the best design is still design 8. Step 12 is the last optimization step performed.

The iteration histories of the thickness t_1, the chordwise extension of the spar, and the tip sweep angle Λ are shown in Figs. 12, 13, and 14, respectively. The tip sweep angle corresponding to the best design is $\Lambda = 9$ deg.

Computational Requirements

All the CPU time mentioned in this section refer to an IBM 3090-200 computer. Each precise aeroelastic analysis required three or four iterations of quasilinearization.[15] Each iteration of quasilinearization required 80–110 CPU s for a straight blade and 140–180 CPU s for a swept tip blade. Because it is a variable step, Adams-Bashforth technique was used to integrate the equations of motion; the exact CPU time required to complete an iteration of quasilinearization was problem dependent.

The remaining portions of a complete optimization step—namely, the calculation of the cross-sectional properties of the blade, the calculation of the vertical hub shears from the aeroelastic response of the blade, the derivation of the polynomial approximations to objective function and behavior constraints, and the solution of the approximate constrained optimization problem—required an average *total* of 1–2 CPU s.

Conclusions and Recommendations

The main conclusions obtained in the present study are summarized below. Their application to the structural optimization of a helicopter blade should be limited by the assumptions used in obtaining the numerical results presented in this study.

1) The optimum design procedure described in this study is very efficient and can produce improved designs with a very limited number of precise analyses. The method of constructing the approximate problem is such that previously conducted aeroelastic analyses can be reused in a new optimization problem. For example, if an optimization study is preceded by a parametric study in which the effect of various combinations of blade design parameters is examined, all the aeroelastic analyses performed for the parametric study can be reutilized in the optimization study. This is not possible when the approximate problem is built from Taylor series expansions.

2) The results of the optimization are quite sensitive to the aeroelastic stability margins required of the blade. In the optimization of case 2, changing the aeroelastic stability constraints, from simply requiring that the blade be stable in hover to requiring that the stability margins be maintained during the course of the optimization, reduced the gains in n/rev vibration levels by more than 50%.

3) The introduction of tip sweep can reduce the n/rev vertical hub shears beyond the level that can be obtained by just modifying the mass and stiffness distributions of the blade.

4) The optimization process described in this study would greatly benefit from improved and more accurate ways of building the polynomial approximations to objective function and behavior constraints. This could be accomplished by deriving analytical gradient information at a fraction of the cost of one aeroelastic analysis, or by identifying appropriate intermediate design variables that would make the polynomial approximations more accurate. For example, polynomial expansions in terms of reciprocal blade section properties might be used in place of cross-sectional dimensions.

Acknowledgments

A considerable part of this work was supported by NASA Ames Research Center, Moffett Field, CA, under Grant NAG 2-226, grant monitor Dr. H. Miura and was done during the first author's stay at UCLA. The use of the University of Maryland Computer Science Center, where some of the numerical results were computed, is hereby acknowledged.

References

[1]Shanthakumaran, P., "Optimum Design of Rotor Blades for Vibration Reduction in Forward Flight," Ph.D. Dissertation, Univ. of California, Los Angeles, CA, 1982.

[2]Friedmann, P. P., "Application of Modern Structural Optimization of Vibration Reduction in Rotorcraft," *Vertica*, Vol. 9, No. 4, 1985, pp. 363-373.

[3]Miura, H., "Application of Numerical Optimization Methods to Helicopter Design Problems—A Survey," *Vertica*, Vol. 9, No. 2, 1985, pp. 141-154.

[4]Celi, R., and Friedmann, P. P., "Aeroelastic Modeling of Swept Tip Rotor Blades Using Finite Elements," *Journal of the American Helicopter Society*, Vol. 33, No. 2, April 1988, pp. 43-52.

[5]Friedmann, P. P., and Shanthakumaran, P., "Aeroelastic Tailoring of Rotor Blades for Vibration Reduction in Forward Flight," AIAA Paper 83-0914, *Proceedings of the AIAA/AHS/ASCE/AHS 24th Structures, Structural Dynamics, and Materials Conference*, Lake Tahoe, NV, Vol. 2, May 1983, pp. 344-359.

[6]Friedmann, P. P., and Shanthakumaran, P., "Optimum Design of Rotor Blades for Vibration Reduction in Forward Flight," *Journal of the American Helicopter Society*, Vol. 29, No. 4, Oct. 1984, pp. 70-80.

[7]Peters, D. A., Rossow, M. P., Korn, A., Ko, T., "Design of Helicopter Rotor Blades for Optimum Dynamic Characteristics," *Computers and Mathematics with Applications*, Vol. 12A, No. 1, 1986, pp. 85-109.

[8]Davis, M. W., and Weller, W. H., "Application of Design Optimization Techniques to Rotor Dynamics Problems," *Journal of the American Helicopter Society*, Vol. 33, No. 3, July 1988, pp. 42-50.

[9]Schmit, L. A., Jr., and Miura, H., "Approximation Concepts for Efficient Structural Synthesis," NASA CR-2552, 1976.

[10]Schmit, L. A., Jr., "Structural Synthesis—Its Genesis and Development," *AIAA Journal*, Vol. 18, No. 10, 1981, pp. 1249-1263.

[11]Lim, J., and Chopra, I., "Design Sensitivity Analysis for an Aeroelastic Optimization of a Helicopter Blade," *Proceedings of the AIAA Dynamics Specialists Conference, Part 2B*, Monterey, CA, April 1987, pp. 1093-1102.

[12]Straub, F. K., and Friedmann, P. P., "Application of the Finite Element Method to Rotary Wing Aeroelasticity," NASA CR-165854, Feb. 1982.

[13]Celi, R., and Friedmann, P. P., "Rotor Blade Aeroelasticity in Forward Flight with an Implicit Aerodynamic Formulation," *AIAA Journal*, Vol. 26, No. 12, Dec. 1988, pp. 1425-1433.

[14]Friedmann, P. P., and Kottapalli, S. B. R., "Coupled Flap-Lag-Torsional Dynamics of Hingeless Rotor Blaes in Forward Flight," *Journal of the American Helicopter Society*, Vol. 27, Oct. 1982, pp. 28-36.

[15]Celi, R., "Aeroelasticity and Structural Optimization of Helicopter Rotor Blades With Swept Tips," Ph.D. Dissertation, Mechanical, Aerospace, and Nuclear Engineering Dept., Univ. of California, Los Angeles, CA, 1987.

[16]Vanderplaats, G. N., "Approximation Concepts for Numerical Airfoil Optimization," NASA TP-1370, March 1979.

[17]Vanderplaats, G. N., *Numerical Optimization Techniques for Engineering Design, With Applications*, McGraw-Hill, NY, 1984, pp. 211-215.

[18]Vanderplaats, G. N., and Moses, F., "Structural Optimization by Methods of Feasible Directions," *Journal of Computers and Structures*, Vol. 3, July 1973, pp. 739-755.

[19]Vanderplaats, G. N., "CONMIN—A FORTRAN Program for Constrained Function Minimization; User's Manual," NASA TM X-62,282, Aug. 1973.

[20]Prouty, R. W., *Helicopter Performance, Stability and Control*, PWS Publishers, Boston, MA, 1986.